Zak phases of chiral photonic crystals designed via transformation optics

Ting Wai Lau [1], Yong-liang Zhang,[1,2,3] and Kin Hung Fung [1,*]
[1]*Department of Applied Physics, The Hong Kong Polytechnic University, Hong Kong, China*
[2]*Department of Physics, Hong Kong Baptist University, Hong Kong, China*
[3]*SKLSM, Institute of Semiconductors, Chinese Academy of Sciences, Beijing 100083, China*

(Received 9 April 2021; revised 24 July 2021; accepted 11 August 2021; published 30 August 2021)

We study a class of inhomogeneous chiral photonic crystals with topologically nontrivial bands and edge modes using the approach of non-coordinate transformation optics. By transforming the chiral photonic crystals into achiral binary photonic crystals, the closed-form solutions to the photonic bands of the chiral photonic crystals are obtained. We show that the topological edge modes of these chiral photonic crystals can be accurately predicted by the Zak phases developed from the topological band theory for achiral binary photonic crystals.

DOI: 10.1103/PhysRevB.104.064312

I. INTRODUCTION

Transformation optics and several theoretical extensions have attracted intensive research interest since the pioneering works of Pendry *et al.* [1] and Leonhardt [2] in 2006. On the basis of the form invariance of Maxwell's equations under coordinate transformation, the light beam in the transformed space will still follow the original trajectory corresponding to its original coordinates. In order words, the trajectory of light in the transformed space can be controlled by adjusting the Jacobian matrix, so that the difficulties in the designs of those materials can be easily overcome [3]. Notable applications include the designs of invisible cloaks [2–4], polarization splitter [5], and extreme plasmonics [6].

Chiral media have rarely been studied using transformation optics [7]. In bianisotropic (chiral) media, **D** and **B** fields are linked to both **E** and **H** fields through complex constitutive relations with cross couplings between electric and magnetic fields. In order to transform chiral into simple media, standard coordinate transformation optics can no longer be used because of the complicated constitutive relations and a non-coordinate transformation method must be considered [7]. Instead of the trajectory of light, optical activities attributed to chirality can be controlled by the flexibility of the transformation matrix. The coupling of the fields in the constitutive relations can provide a wider parameter space for realizing different topological phases [8]. To the best of our knowledge, transformation optics has not been applied to topological photonics.

In this paper, we consider topological phases of chiral photonic crystals associated with Zak phases, where the concept of "photon spin" [9,10] is not required. As one of the topological invariants in topological photonics, Zak phases of one-dimensional (1D) isotropic layered photonic crystals with inversion symmetries has been widely discussed in recent years [11,12]. So far, the theories of Zak phases have not been applied to one-dimensional (1D) bianisotropoic chiral photonic crystals. Here the technique of transformation optics is employed to design 1D topological photonic crystals with nonzero optical activity. By choosing suitable parameters, topological edge states of a system composed of the designed chiral photonic crystal and a simple isotropic binary photonic crystal can be predicted via the topological theories of isotropic layered photonic crystals.

This paper is organized as follows. In Sec. II A, we demonstrate how to transform a chiral medium with nonzero chirality parameter to a simple medium with zero chirality using a 4×4 transformation matrix. In Sec. II B, we construct a chiral photonic crystal with the transformed chiral material as its unit cell. In Secs. II C and II D, the Zak phases and the topological edge states of the chiral photonic crystal are examined.

II. RESULTS

A. Eliminating chirality via transformation optics

To ensure the chirality parameter can be eliminated during the transformation, we consider the transformation from a bianisotropic medium with isotropic chirality to a simple anisotropic medium. In such transformation, the chiral medium is considered as the "physical space" (x, y, z), and the simple anisotropic medium is considered as the "virtual space" (x', y', z'). We start with considering continuous waves of angular frequency ω propagating along the z axis. The transverse components of the electromagnetic (EM) fields in the frequency domain can be expressed as $\mathbf{F} = (E_x, E_y, Z_0 H_x, Z_0 H_y)^T$, where Z_0 is impedance in a vacuum. Maxwell's equations in the frequency domain can be written in a differential matrix form [13]:

$$\frac{d}{dz}\mathbf{F}(z) = \frac{i\omega}{c}[\mathbf{M}(z) + i\mathbf{K}(z) + \mathbf{L}(z)]\mathbf{F}(z), \tag{1}$$

where c is the speed of light in vacuum, and the 4×4 matrices **M** and **K** are given by

$$\mathbf{M} = \begin{pmatrix} 0 & 0 & \mu_{21} & \mu_{22} \\ 0 & 0 & -\mu_{11} & -\mu_{12} \\ -\varepsilon_{21} & -\varepsilon_{22} & 0 & 0 \\ \varepsilon_{11} & \varepsilon_{12} & 0 & 0 \end{pmatrix} \tag{2}$$

*khfung@polyu.edu.hk

and

$$\mathbf{K} = \kappa \begin{pmatrix} 0 & 1 & 0 & 0 \\ -1 & 0 & 0 & 0 \\ 0 & 0 & 0 & 1 \\ 0 & 0 & -1 & 0 \end{pmatrix}. \tag{3}$$

In the above equations, chirality parameter $\kappa(\omega, z)$, relative dielectric permittivity tensor $\varepsilon_{ij}(\omega, z)$, and relative magnetic permeability tensors $\mu_{ij}(\omega, z)$ (with $i, j = 1, 2, 3$) are allowed to be dependent on the frequency ω and position z. The details of the matrix $\mathbf{L}$ are shown in Appendix A for clarity.

Although Eq. (1) can be solved numerically, we seek analytical solutions through transformation. For demonstration, we set $\varepsilon_{13} = \varepsilon_{23} = \varepsilon_{31} = \varepsilon_{32} = 0$ and $\mu_{13} = \mu_{23} = \mu_{31} = \mu_{32} = 0$ in both the physical spaces so that $\mathbf{L}(\omega, z) = \mathbf{0}$ and $E_z = H_z = 0$. In the virtual space, we further choose the permittivity and permeability tensors to be homogeneous and nondispersive so that the EM waves in the virtual space are just plane waves. The transformation from the physical space to the virtual space is expected to eliminate the chirality parameter (i.e., $\kappa = 0$ in the virtual space).

By adding prime ($'$) to associated symbols in Eq. (1), Maxwell's equations in the virtual space can be written as

$$\frac{d}{dz'}\mathbf{F}'(\omega, z') = \frac{i\omega}{c}\,\mathbf{M}'(\omega, z') + \mathbf{L}'(\omega, z')\mathbf{F}'(\omega, z'), \tag{4}$$

where $\mathbf{L}'(\omega, z') = \mathbf{0}$ in this situation. The mapping between the fields in the physical and virtual spaces is given by $\mathbf{F}'(\omega, z') = \mathbf{R}(\omega, z)\,\mathbf{F}(\omega, z)$, where $\mathbf{R}(\omega, z)$ is a noncoordinate transformation matrix. The transformation we obtained is the Oseen transformation [14]:

$$\mathbf{R}(\omega, z) = \begin{pmatrix} \cos\theta & \sin\theta & 0 & 0 \\ -\sin\theta & \cos\theta & 0 & 0 \\ 0 & 0 & \cos\theta & \sin\theta \\ 0 & 0 & -\sin\theta & \cos\theta \end{pmatrix}, \tag{5}$$

where

$$\theta(\omega, z) = \frac{\omega}{c}\int_{z_0}^{z} \kappa(\omega, u)\, du, \tag{6}$$

where z_0 is the initial point of the system and $z = z'$ is chosen due to its arbitrariness (see Appendix B). The transformation is a rotation of the x-y planes about the z axis, and the angle of rotation $\theta(\omega, z)$ is dependent on frequency in general. Optical rotation contributed by chirality can be completely eliminated through the transformation. In other words, the angle of rotation in the physical space can be controlled by the transformation matrix.

It should be noted that the transformation matrix is allowed to be dependent on frequency to account for frequency-dependent optical activities [15]. We should also emphasize that Oseen transformation is not the only transformation. If $\mathbf{L} \neq \mathbf{0}$, Oseen transformation is not enough to eliminate the chirality parameter. Since constant electromagnetic parameters in the virtual space (achiral medium) are considered, the wave solution in the physical space (isotropic chiral medium) can be expressed as

$$\begin{aligned}\mathbf{F}(\omega, z) &= \mathbf{R}^{-1}(\omega, z)\,\mathbf{F}'(\omega, z) \\ &= \mathbf{R}^{-1}(\omega, z)\,\exp\left[\frac{i\omega\Delta z}{c}\mathbf{M}'\right]\mathbf{F}(\omega, z_0),\end{aligned} \tag{7}$$

with $\Delta z = z - z_0$ and $\mathbf{R}^{-1}(\omega, z)$ becomes a 4×4 identity matrix at $z = z_0$. For convenience, the permittivity and permeability tensors in the virtual space are further supposed to be $\mathrm{diag}(\varepsilon'_{11}, \varepsilon'_{22}, \varepsilon'_{33})$ and $\mathrm{diag}(\mu'_{11}, \mu'_{22}, \mu'_{33})$, respectively. Thus, the permittivity tensor in the physical space is

$$\boldsymbol{\varepsilon}' = \frac{1}{\det\mathbf{A}}\,\mathbf{A}\boldsymbol{\varepsilon}(z)\mathbf{A}^T$$

$$\Rightarrow \boldsymbol{\varepsilon}(z) = \begin{pmatrix} C_1 + C_2\cos 2\theta & C_2\sin 2\theta & 0 \\ C_2\sin 2\theta & C_1 - C_2\cos 2\theta & 0 \\ 0 & 0 & \varepsilon'_{33} \end{pmatrix}, \tag{8}$$

where

$$C_1 = \frac{\varepsilon'_{11} + \varepsilon'_{22}}{2}, \quad C_2 = \frac{\varepsilon'_{11} - \varepsilon'_{22}}{2}.$$

$\mathbf{A}$ is the transformation matrix in the three-dimensional space, for example, $\mathbf{E}' = [\mathbf{A}^T]^{-1}\mathbf{E}$. The relation of $\mathbf{R}$ and $\mathbf{A}$ can be written as $\mathbf{R}(\omega, z) = \mathbf{I}_{2\times 2} \otimes [[(\mathbf{A}^T)^{-1}]_{ab}]$, where $a, b = 1, 2$. More details about the transformation can be found in Appendix B. Also, the permeability tensor can be found by simply replacing ε'_{ij} with μ'_{ij}.

It can be argued that the permittivity and permeability tensors including $\cos 2\theta(\omega, z)$ and $\sin 2\theta(\omega, z)$ may be difficult to realize in materials. This can be resolved by two methods. First, we can regard the frequency of the incident light as fixed during the transformation (say ω_1) so that the transformation matrix $\mathbf{R}$ only depends on z. As a result, there is an analytical wave solution to the designed chiral material only when the frequency of the incident light equals ω_1. Second, we can choose the chirality parameter as $\kappa(\omega, z) \to \kappa_0(z)/\omega$ so that θ is independent of ω, and the analytical solution is valid for a wider frequency range. The second method is taken into consideration in the following.

B. Solutions to chiral photonic crystals

The technique of transformation optics has been used to design an inhomogeneous chiral material. Instead of the trajectory, the angle of rotation can be controlled by the transformation matrix, whereas there exists functions which are difficult to realize in the electromagnetic parameters. In order that the result can be appropriate for a wider frequency range, an adjustment to the chirality parameter is considered so that $\theta(\omega, z) \to \theta(z)$. Chiral photonic crystals can be formed by repeating the designed chiral material. Hence, $\theta(z)$ will not necessarily be a continuous function through whole space.

The wave solution of the chiral photonic crystal can be found by transfer-matrix method. By Bloch's theorem, the dispersion relation is

$$\mathbf{R}^{-1}(a)\,\exp\left(\frac{i\omega a}{c}\mathbf{M}'\right)\mathbf{F}(\omega, 0) = e^{ik_z a}\mathbf{F}(\omega, 0), \tag{9}$$

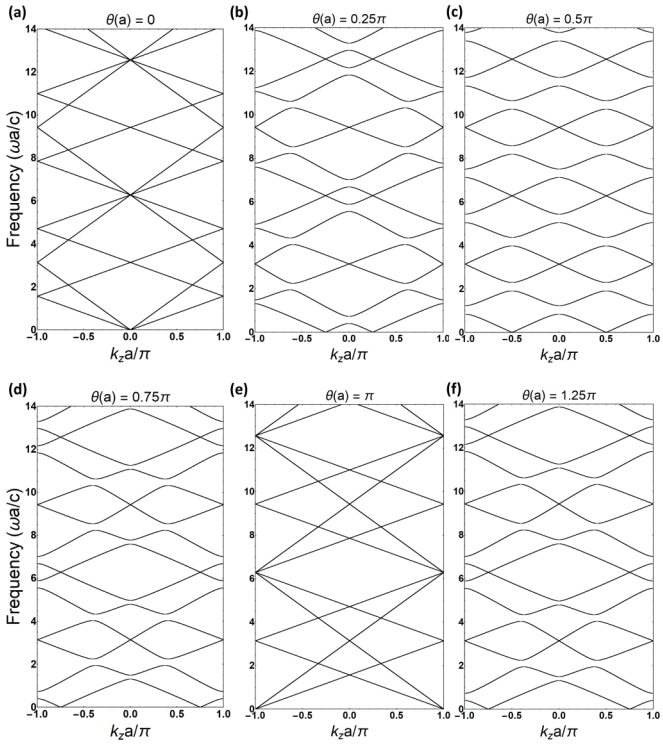

FIG. 1. The band structures of the chiral photonics crystals. $\theta(a)$ is supposed to be $\lim_{z\to a^+}\theta(z)$. The parameters in the virtual space are given by $\varepsilon'_{11}=4$ and $\varepsilon'_{22}=\mu'_{11}=\mu'_{22}=1$, where ε'_{33} can be arbitrary due to $\mathbf{L}'=\mathbf{0}$. Panels (a)–(f) are the band structures of $\theta(a)$ equal to 0, 0.25π, 0.5π, 0.75π, π, and 1.25π respectively. Panel (a) can overlap with panel (e), and panel (b) can overlap with panel (d) if either one of them is shifted left or right by 1.

where a is the length of a unit cell and k_z is the Bloch wave vector. The starting point of the system z_0 is assumed to be 0. According to Eq. (5), the dispersion relation only depends on the angle $\theta(a)\ (\mathrm{mod}\ 2\pi)$ if the permittivity and permeability tensors in the virtual space ($\boldsymbol{\varepsilon}'$ and $\boldsymbol{\mu}'$) are unchanged. In other words, no matter what the functions $\theta(z)$ are, the band structures will still be the same if $\theta(a)\ (\mathrm{mod}\ 2\pi)$ are the same. For this reason, we can simplify our consideration by choosing $\kappa(z)$ as a constant so that $\theta(z)$ becomes a linear function in a unit cell. The structural "twisted" angle of the designed chiral photonic crystal becomes

$$\theta(z)=\theta_{\max}\left(\frac{z}{a}-\left\lfloor\frac{z}{a}\right\rfloor\right), \tag{10}$$

where $\theta_{\max}=\lim_{z\to a^+}\theta(z)$. Floor function is included because θ will be reset to initial value after a unit cell. i.e., $\theta(z+a)=\theta(z)$. Although the property of floor function results in θ equals 0 at $z=a$, $\theta(a)$ will still be used to emphasize the structural angle of a unit cell for convenience and consistency; hence, $\theta(a)$ is supposed to be $\lim_{z\to a^+}\theta(z)=\theta_{\max}$.

The band structures of $\theta(a)=0,\ 0.25\pi, 0.5\pi, 0.75\pi, \pi$, and 1.25π are shown in Fig. 1. The permittivity and permeability tensors in the virtual space are given by $\mathrm{diag}(4, 1, \varepsilon'_{33})$ and identity respectively, where ε'_{33} can be arbitrary because of $\mathbf{L}'=\mathbf{0}$ in this situation. When $\theta(a)=0$, the system is a simple anisotropic and homogeneous material; thus, the band structure in the physical space is no difference from the structure in the virtual space. When $\theta(a)$ increases, the bands split and photonic band gaps appear. The band splitting can be attributed to the existence of chirality [13,16], while the appearance of band gaps is due to the discontinuity of the permittivity tensors. At the lowest frequency, k_z is not equal to 0, which may be due to the validity of our chosen chiral model at low frequencies. According to the one-resonance Condon model, the chirality parameter with single resonant frequency should be expressed as [17]

$$\kappa(\omega,z)=\frac{\omega}{\omega^2-\omega_0^2}\,\kappa_0(z), \tag{11}$$

where ω_0 is the resonant frequency of chirality. In our chiral model, we suppose $\omega\gg\omega_0$ so that $\kappa\propto 1/\omega$. When $\theta(a)$ increases to 0.5π, there appears the largest number of complete photonic band gaps. When $\theta(a)$ further increases, the gaps are closing and the bands further split. When $\theta(a)=\pi$, the photonic band gaps are completely closed and the band structure is shifted to left (or right) by 1 compared to Fig. 1(a). When $\theta(a)$ further increases, the band structure starts returning back to the band structure of $\theta(a)=0$.

The band structures of $\theta(a)$ and $\pi+\theta(a)$ can be overlapped by shifting either one to the left (or right) by 1, and the eigenvectors also follow the shifting, for example, Figs. 1(b) and 1(f). Similar results can be obtained in the regions $\theta(a)\in(0.5\pi,\pi]$ and $[0,0.5\pi)$; for example, Figs. 1(b) and 1(d). Nevertheless, although the band structures found in $\theta(a)\in(0.5\pi,\pi]$ can overlap with the band structure of $\pi-\theta(a)$ by shifting either one to the left (or right) by 1, the eigenvectors are not following the shifting. Consequently, it is adequate that only $\theta(a)\in[0,\pi]$ is considered. The mathematical details are shown in Appendix C. The case of $\theta(a)=\pi/2$ is focused because there appears the largest number of complete photonic band gaps.

C. Zak phases

Zak phase is one of the important topological invariants in 1D photonic systems. If a phenomenon can be linked up with topological invariants, it is possible to claim that the phenomenon is topologically protected (without breaking certain symmetries). The Zak phase of the nth isolated band can be numerically calculated by [11,12]

$$\Phi_n^{\mathrm{Zak}}=i\sum_m \ln\langle\Psi_m|\Psi_{m+1}\rangle+i\,\ln\langle\Psi_f|\Psi_i\rangle, \tag{12}$$

where $|\Psi_m\rangle$ is the normalized eigenstate at the mth Bloch wave vector, $k_z a/\pi=-1+m\Delta k_z a/\pi$. $|\Psi_i\rangle$ and $|\Psi_f\rangle$ are the initial and final eigenstates of the nth isolated band such that the path in momentum space is a closed loop. $|\Psi\rangle$ should directly make use of the eigenvectors obtained in Eq. (9) in principle. However, this is not the case in chiral photonic crystals. In simple isotropic layered photonic crystals, (E_x, H_y) and (E_y, H_x) modes are equivalent, so only either one of the modes needs considering. In contrast, two modes are different and even coupled in bianisotropic medium. Furthermore, the Zak phases calculated by these coupled modes have not been widely discussed. By choosing diagonal permittivity and permeability tensors in the virtual space and $\theta_{\max}=\pi/2$, two

TABLE I. Notation of tensors in the virtual space, physical, and transformed structures.

Tensors	Virtual	Physical	Transformed structure
Dielectric	$\boldsymbol{\varepsilon}'(z')$	$\boldsymbol{\varepsilon}(z)$	$\boldsymbol{\varepsilon}''(z)$
Magnetic	$\boldsymbol{\mu}'(z')$	$\boldsymbol{\mu}(z)$	$\boldsymbol{\mu}''(z)$
Chiral	$\mathbf{0}$	$\kappa(z)\mathbf{I}/\omega$	$\mathbf{0}$

independent modes can be fortunately decoupled after a continuous transformation. The transformation matrix is the same as Eq. (5) but the discontinuous function $\theta(z)$ is replaced by a continuous function $\phi(z)$. On the basis of the Eq. (10), the continuous function can be expressed as

$$\phi(z) = \theta_{\max}\frac{z}{a} = \frac{\pi z}{2a}. \tag{13}$$

In order to distinguish the parameters in the physical space and the new transformed structure, the symbols with double prime ($''$) are used to represent the parameters in the new transformed structure. The notation of the tensors in different spaces are shown in Table I. The permittivity tensor in the transformed structure is

$$\begin{aligned}\boldsymbol{\varepsilon}''(z) &= \frac{1}{\det\mathbf{A}}\mathbf{A}\boldsymbol{\varepsilon}(z)\mathbf{A}^T \\ &= \begin{cases}\mathrm{diag}(\varepsilon'_{11}, \varepsilon'_{22}, \varepsilon'_{33}), & \text{if } \lfloor z/a \rfloor \text{ is odd} \\ \mathrm{diag}(\varepsilon'_{22}, \varepsilon'_{11}, \varepsilon'_{33}), & \text{if } \lfloor z/a \rfloor \text{ is even}\end{cases}.\end{aligned} \tag{14}$$

Again, the permeability tensor in the transformed structure can be found by simply replacing ε'_{ij} with μ'_{ij}. The chirality parameter in transformed structure κ'' returns to 0. The transformed structure is a simple anisotropic binary photonic crystal shown in Fig. 2(a), where the permittivity and permeability tensors of white and black slabs are given by Eq. (14) when $\lfloor z/a \rfloor$ is odd and even respectively. Compared with the original chiral structure, the width of a unit cell (Λ) is double

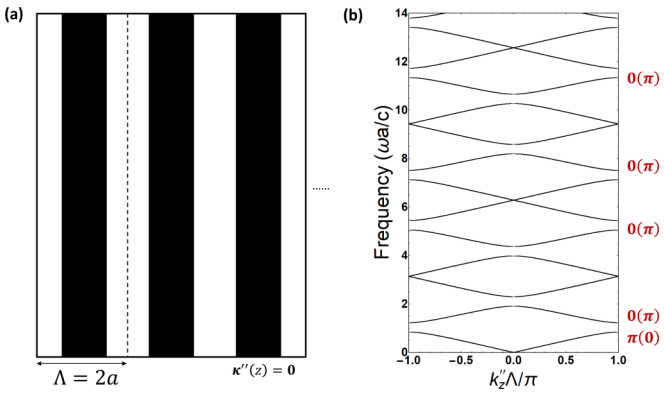

FIG. 2. (a) Schematic of the transformed structure when $\theta(a) = 0.5\pi$ is chosen. The permittivity (and permeability) parameters of white and black slabs are given by Eq. (14) when $\lfloor z/a \rfloor$ is odd and even respectively. A center of a white slab is chosen as an origin of the system and the width of a unit cell Λ equals $2a$. (b) The band structure of the transformed anisotropic binary photonic crystal. The parameters in the virtual space are given by $\varepsilon'_{11} = 4$ and $\varepsilon'_{22} = \mu'_{11} = \mu'_{22} = 1$. The Zak phases calculated by $|\psi_{x''}\rangle$ ($|\psi_{y''}\rangle$) are labeled near the corresponding isolated band.

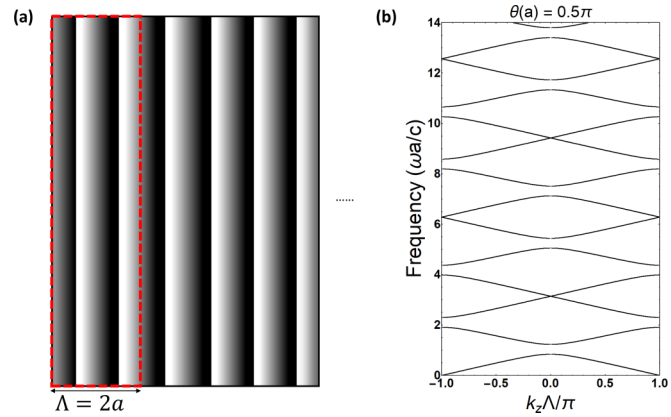

FIG. 3. (a) The structure of the chiral photonic crystal by choosing $\theta(a) = 0.5\pi$, where $\theta(a) = \lim_{z\to a^+}\theta(z)$. Two unit cells are regarded as a period and the center of a unit cell is chosen as an origin for fear of losing the generality. Color gradient is used to represent the parameters are gradually changing along the z direction. (b) The band structure of the chiral photonic crystal by considering two unit cells as a period. The parameters in the virtual space are given by $\varepsilon'_{11} = 4$ and $\varepsilon'_{22} = \mu'_{11} = \mu'_{22} = 1$.

to be $2a$ and z-inversion symmetry exists, where the inversion centers are at the center in each slab.

To ensure that the Zak phases can be quantized as usual, a center of a white slab is chosen as an origin of the system. The dispersion relation of the transformed structure can be found by transfer-matrix method:

$$\begin{aligned}&e^{ik''_z\Lambda}\mathbf{F}''(\omega, 0) \\ &= \left(\frac{i\omega a}{2c}\mathbf{M}''_w\right)\exp\left(\frac{i\omega a}{c}\mathbf{M}''_b\right)\exp\left(\frac{i\omega a}{2c}\mathbf{M}''_w\right)\mathbf{F}''(\omega, 0),\end{aligned} \tag{15}$$

where $\mathbf{M}''_w$ and $\mathbf{M}''_b$ are the constant matrices following Eq. (2). The subscripts w and b represent white and black slabs respectively. k''_z is the Bloch wave vector of the transformed structure. The corresponding band structure is shown in Fig. 2(b), where the parameters in the virtual space are given by $\varepsilon'_{11} = 4$ and $\varepsilon'_{22} = \mu'_{11} = \mu'_{22} = 1$. The band structure shows two independent eigenmodes are degenerated.

To have a valid comparison between the original and transformed structures, two unit cells of the chiral photonic crystal are considered as a period ($\Lambda = 2a$) and a center of a unit cell is chosen as an origin of the system. Schematic of the chiral photonic crystal and the band structure are shown in Fig. 3. The band structure calculated by using a single unit cell as a period is already shown in Fig. 1(c). By comparing Figs. 2(b) and 3(b), the band structures can be overlapped via shifting either one to the left (or right) by 1, i.e.,

$$\frac{k_z\Lambda}{\pi} = \frac{k''_z\Lambda}{\pi} + (2s - 1), \tag{16}$$

where s is an integer for controlling the wave vector within the range of $[-1, 1]$. Since the eigenstates at $k_z\Lambda/\pi$ (in the original structure) are the same as at $k''_z\Lambda/\pi + (2s - 1)$ (in the transformed structure), the Zak phases of the corresponding bands in the two-band structures are the

same. If we rearrange the eigenvectors in the from $\mathbf{F}'' = (E''_{x''},\ Z_0 H''_{y''},\ E''_{y''},\ -Z_0 H''_{x''})^T$, the operator in Eq. (15) becomes a block-diagonal matrix composed of two 2×2 matrices. Consequently, the eigenstates in the transformed structure are decoupled to $(E''_{x''},\ Z_0 H''_{y''})^T$ and $(E''_{y''},\ -Z_0 H''_{x''})^T$, which will be denoted as $|\psi_{x''}\rangle$ and $|\psi_{y''}\rangle$ modes respectively for clear presentation. Similarly, $|\psi_x\rangle$ and $|\psi_y\rangle$ will be used to represent the same modes in the physical space.

In simple isotropic layered photonic crystals, only either of the modes needs considering because of $|\psi_x\rangle$ equivalent to $|\psi_y\rangle$; however, both of the modes have to be considered in anisotropic binary photonic crystals since $|\psi_x\rangle$ and $|\psi_y\rangle$ are not necessarily equivalent. When $|\psi_{x''}\rangle$ (or $|\psi_{y''}\rangle$) mode is considered, the transformed structure can be further regarded as an isotropic AB (or BA) layered photonic crystal with the parameters $\varepsilon_A = \varepsilon'_{11}$, $\varepsilon_B = \varepsilon'_{22}$, $\mu_A = \mu'_{22}$, and $\mu_B = \mu'_{11}$. Thus, the topological theories of 1D binary photonic crystals can be totally applied. Simple isotropic AB layered photonic crystals always have two different inversion centers, centers of slabs A and B. If the Zak phase of an isolated band is $0(\pi)$ by choosing one of the inversion centers as an origin, the Zak phase of the same band must be $\pi(0)$ when another inversion center is chosen [11]. As a result, in our transformed photonic crystal, if the Zak phase calculated by $|\psi_{x''}\rangle$ mode is $0(\pi)$, the Zak phase of the same band calculated by $|\psi_{y''}\rangle$ mode will be $\pi(0)$. In other words, one isolated band has two different Zak phases. The results are also shown in Fig. 2(b). There is a remark that the Zak phase at the 0th band is determined by the following equation due to the degenerated point existed at the $\omega = 0$ [11]:

$$\exp\left(\Phi_0^{\mathrm{Zak}}\right) = \mathrm{sgn}\left[1 - \frac{\varepsilon_A \mu_B}{\varepsilon_B \mu_A}\right]. \tag{17}$$

D. Existence of interface states

The designed chiral photonic crystal can be transformed to a simple anisotropic binary photonic crystal. If either $|\psi_{x''}\rangle$ or $|\psi_{y''}\rangle$ mode is considered, it can further be regarded as a simple isotropic AB or BA layered photonic crystal respectively. Hence, the theories developed from isotropic binary photonic crystals can be applied. For clarity, we respectively name the simple anisotropic and isotropic binary photonic crystals to be type I and type II achiral photonic crystals (shown in Table II). Interface states of a system composed of our designed chiral photonic crystal and a type II achiral photonic crystal are examined. In order to guarantee midgap positions of the photonic crystals are the same, the optical path lengths should be equivalent [11,12], i.e.,

$$(\sqrt{\varepsilon'_{11}} + \sqrt{\varepsilon'_{22}})a = n_A d_A + n_B d_B, \tag{18}$$

TABLE II. Types of the achiral binary photonic crystals used in this paper.

Constituent	Type
Anisotropic	Type I achiral photonic crystal
Isotropic	Type II achiral photonic crystal

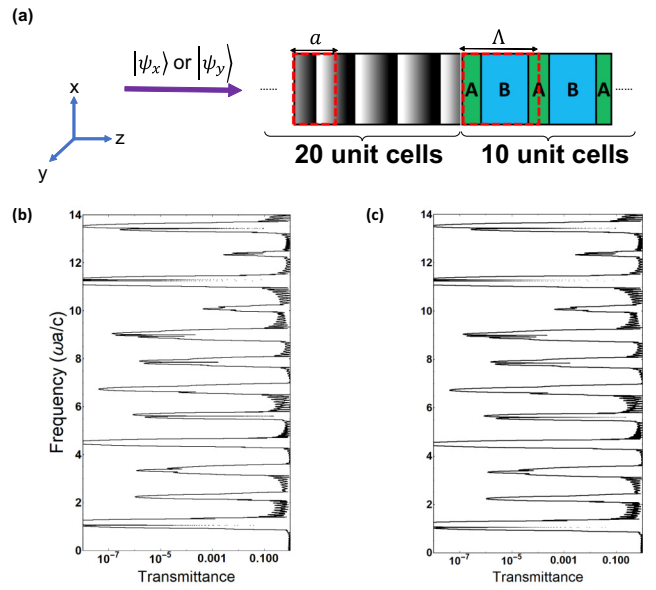

FIG. 4. Calculation of transmittance through the tested finite system. The system is composed of 20 unit cells of the designed chiral photonic crystal on the left and 10 unit cells of a type II achiral photonic crystal on the right. The parameters of the chiral photonic crystal in the virtual space are given by $\varepsilon'_{11} = 3.23$ and $\varepsilon'_{22} = \mu'_{11} = \mu'_{22} = 1$. In the type II achiral photonic crystal, green and blue slabs are slabs A and B respectively. The parameters of the slabs are given by $\varepsilon_A = 4.2$, $\varepsilon_B = \mu_A = \mu_B = 1$, $d_A = 0.76a$, and $d_B = 1.24a$. [(b), (c)] The transmission spectra of the system calculated by $|\psi_x\rangle$ and $|\psi_y\rangle$ modes respectively. The spectra are the same.

where n_A and n_B are the refractive indices of slabs A and B of a type II achiral photonic crystal; also, d_A and d_B are the widths of slabs A and B respectively. Without loss of generality, the method of choosing a unit cell is the same as Figs. 2(a) and 3(a). The tested system is composed of 20 unit cells of our chiral photonic crystal on the left and 10 unit cells of a type II achiral photonic crystal on the right, where the widths of a unit cells of our chiral photonic crystal and the type II achiral photonic crystal are a and $2a$ respectively. The system is shown in Fig. 4(a). The transmission spectra of the system calculated by $|\psi_x\rangle$ and $|\psi_y\rangle$ modes are shown in Figs. 4(b) and 4(c). The parameters of the chiral photonic crystal in the virtual space are given by $\varepsilon'_{11} = 3.23$ and $\varepsilon'_{22} = \mu'_{11} = \mu'_{22} = 1$, and the parameters of the type II achiral photonic crystal are given by $\varepsilon_A = 4.2$ and $\varepsilon_B = \mu_A = \mu_B = 1$. The transmission spectra are the same and interface states exist in the 1st, 3rd, 5th, 7th, 8th, 10th, 11th, and 12th gaps. Owing to a conformal mapping from the designed chiral photonic crystal to a type I achiral photonic crystal, the system can be considered as a composition of 10 unit cells of the transformed type I achiral photonic crystal on the left and 10 unit cells of the type II achiral photonic crystal on the right. Since a center of a unit cell is chosen as an origin, the incident fields ($|\psi_x\rangle$ or $|\psi_y\rangle$) are rotated by 45° when the transformed system is considered. Furthermore, $|\psi_x\rangle$ (or $|\psi_x\rangle$) can always be decomposed into a linear combination of $|\psi_{x''}\rangle$ and $|\psi_{y''}\rangle$. Consequently, the transmission spectrum of $|\psi_x\rangle$ or $|\psi_y\rangle$ is the sum of the transmission spectra of $|\psi_{x''}\rangle$ and $|\psi_{y''}\rangle$, which is the reason

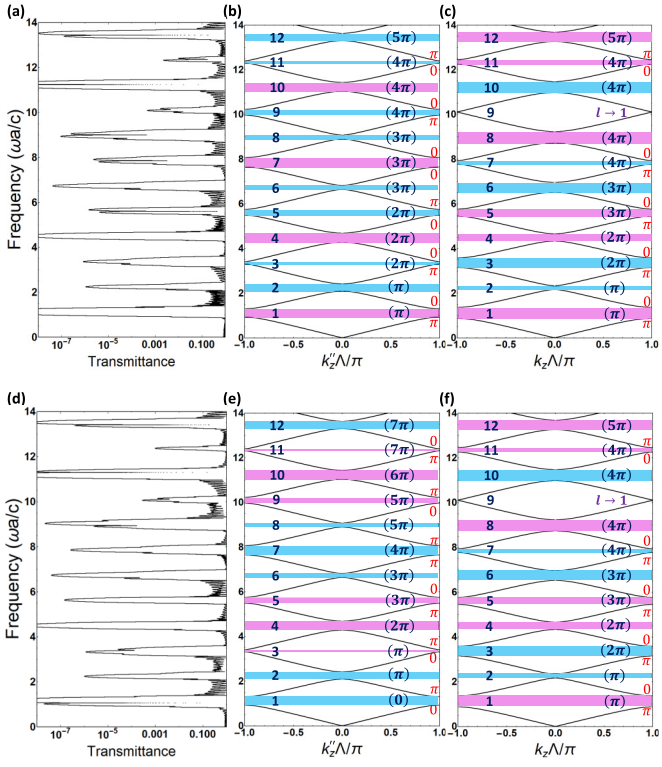

FIG. 5. [(a), (d)] The transmission spectra calculated by $|\psi_x\rangle$ and $|\psi_y\rangle$ modes respectively. The system is composed of 10 unit cells of a transformed type I achiral photonic crystal on the left and 10 unit cells of a type II achiral photonic crystal on the right. The parameters of the transformed type I achiral photonic crystal in the virtual space are given by $\varepsilon'_{11} = 3.23$ and $\varepsilon'_{22} = \mu'_{11} = \mu'_{22} = 1$, and the parameters of the type II achiral photonic crystal are given by $\varepsilon_A = 4.2$, $\varepsilon_B = \mu_A = \mu_B = 1$, $d_A = 0.76a$, and $d_B = 1.24a$. [(b), (e)] The band structures of the transformed type I achiral photonic crystal. [(c), (f)] The band structure of the type II achiral photonic crystal. The band structures calculated by $|\psi_x\rangle$ and $|\psi_y\rangle$ modes are the same. The magenta and cyan strips represent the gaps with $\zeta > 0$ and $\zeta < 0$ respectively. The Zak phase of each band are denoted near the band and the number in the brackets are the sum of the Zak phases below the gaps.

why the transmission spectra, Figs. 4(b) and 4(c), are the same.

The positions of interface states can also be predicted. As the transformed type I achiral photonic crystal can be regarded as a type II achiral photonic crystal when either $|\psi_{x''}\rangle$ or $|\psi_{y''}\rangle$ mode is considered, the system can also be regarded as a composition of 10 unit cells of a type II achiral photonic crystal on the left and 10 unit cells of a type II achiral photonic crystal on the right. The existence of interface states of a system composed of two type II achiral photonic crystals can be predicted by the signs of the surface impedance:

$$\mathrm{sgn}[\zeta^{(n)}] = (-1)^{n+l} \exp\left(i \sum_{p=0}^{n-1} \Phi_p^{\mathrm{Zak}} \right), \tag{19}$$

where the integer l is the number of degenerated points below the nth band gap. Interface states appear if $\mathrm{sgn}[\zeta^{(n)}]$ of two connected type II achiral photonic crystals are opposite in common gaps. The transmission spectra of $|\psi_{x''}\rangle$ and $|\psi_{y''}\rangle$ modes are shown in Figs. 5(a) and 5(d). The band structures of our transformed type I achiral and the type II achiral photonic crystals are shown in Figs. 5(b) and 5(c) [also in Figs. 5(e) and 5(f)] respectively. The parameters of the type I and the type II achiral photonic crystals are the same as the parameters used in Fig. 4. The band structures shown in Figs. 5(b) and 5(e) are the same but the Zak phases are different by π. Magenta strip represents $\mathrm{sgn}[\zeta^{(n)}] > 0$; otherwise, the strip is cyan. The interface state exists if $\mathrm{sgn}[\zeta^{(n)}]$ at the common gaps are opposite. In the transmission spectrum of $|\psi_{x''}\rangle$ mode, the interface states exist in the 5th, 7th, 8th, 10th, 11th, and 12th gaps; in the transmission spectrum of $|\psi_{y''}\rangle$ mode, the interface states exist in 1st, 3rd, 8th, 10th, and 12th gaps. Therefore, in the transmission spectrum of $|\psi_x\rangle$ or $|\psi_y\rangle$ mode, interface states of a system composed of our chiral photonic crystal and the type II achiral photonic crystal will exist in the 1st, 3rd, 5th, 7th, 8th, 10th, 11th, and 12th gaps. The prediction is consistent with the transmission spectra shown in Figs. 4(b) and 4(c).

III. CONCLUSIONS

A class of inhomogeneous chiral photonic crystals with topologically nontrivial bands and edge modes are studied by using the technique of transformation optics. Due to the complicated constitutive relations of chiral media, a non-coordinate transformation optics is developed so that the chirality parameter can be eliminated during transformation. Instead of paths of light, the optical activities attributed to chirality are controlled by the transformation matrix. In this paper, 1D systems and simple electromagnetic tensors are considered such that we can easily obtain the transformation matrix. According to Ref. [7], the technique of transformation optics is also available for more general cases, including 3D systems; however, the calculation for finding the transformation matrix will become extremely complicated. If the permittivity and permeability tensors in the virtual space are diagonal, the designed chiral photonic crystal can be transformed to an anisotropic binary photonic crystal and corresponding Zak phases can be obtained. The predictions of topological edge modes by the Zak phases are verified by transmittance calculations. Finally, our results of the Zak phases not only are of fundamental interests in the analysis of topological bands and the interface states but also can be used to analyze a variety of novel phenomena in photonic crystals. For instance, our calculation is useful for the design of the interface states in different kinds of finite chiral photonic crystals as in achiral distributed Bragg reflectors [18] or even topologically nontrivial chiral Fabry-Perot resonator. Moreover, the non-coordinate transformation method used here can be extended to deal with optical switching [19], nonlinear topological modes [20], and gap solitons [21] in nonlinear chiral photonic crystals.

ACKNOWLEDGMENTS

This work was supported by the Hong Kong Research Grants Council (C6013-18G and AoE/P-02/12). We thank

C. T. Chan, Jensen Li, Wang Tat Yau, and Kai Fung Lee for fruitful discussions.

APPENDIX A: DIFFERENTIAL EQUATIONS FOR 1D ISOTROPIC CHIRAL MEDIUM

We consider a stack of anisotropic layers that are homogeneous in x and y directions, and suppose the incident light propagates along the z direction. We also suppose the macroscopic electric and magnetic fields are time harmonic; hence, the constitutive relations are

$$\mathbf{D}(z) = \varepsilon_0 \boldsymbol{\varepsilon}(z)\mathbf{E}(z) - i\sqrt{\mu_0\varepsilon_0}\,\kappa(z)\mathbf{H}(z), \tag{A1a}$$

$$\mathbf{B}(z) = \mu_0 \boldsymbol{\mu}(z)\mathbf{H}(z) + i\sqrt{\mu_0\varepsilon_0}\,\kappa(z)\mathbf{E}(z), \tag{A1b}$$

where it is understood that all variables are also dependent on frequency ω. After applying Faraday's and Ampere's laws, we get

$$\begin{pmatrix} \frac{d}{dz} & \frac{\omega\kappa}{c} \\ -\frac{\omega\kappa}{c} & \frac{d}{dz} \end{pmatrix}\begin{pmatrix} E_x \\ E_y \end{pmatrix} = i\omega\mu_0\begin{pmatrix} \mu_{21}H_x + \mu_{22}H_y + \mu_{23}H_z \\ -\mu_{11}H_x - \mu_{12}H_y - \mu_{13}H_z \end{pmatrix},$$

$$\begin{pmatrix} \frac{d}{dz} & \frac{\omega\kappa}{c} \\ -\frac{\omega\kappa}{c} & \frac{d}{dz} \end{pmatrix}\begin{pmatrix} H_x \\ H_y \end{pmatrix} = i\omega\varepsilon_0\begin{pmatrix} -\varepsilon_{21}E_x - \varepsilon_{22}E_y - \varepsilon_{23}E_z \\ \varepsilon_{11}E_x + \varepsilon_{12}E_y + \varepsilon_{13}E_z \end{pmatrix},$$

and

$$H_z + \frac{i\kappa}{\mu_{33}}\sqrt{\frac{\varepsilon_0}{\mu_0}}E_z = -\frac{1}{\mu_{33}}[\mu_{31}H_x + \mu_{32}H_y],$$

$$H_z - \sqrt{\frac{\varepsilon_0}{\mu_0}}\frac{\varepsilon_{33}}{i\kappa}E_z = \sqrt{\frac{\varepsilon_0}{\mu_0}}\frac{1}{i\kappa}[\varepsilon_{31}E_x + \varepsilon_{32}E_y].$$

By expressing E_x and H_z in terms of x and y components, Eq. (1) can be formed. The 4×4 matrix $\mathbf{L}$ can be separated into $\mathbf{L_1} + i\mathbf{L_2}$. $\mathbf{L_1}$ and $\mathbf{L_2}$ are antiblock diagonal and block diagonal matrices:

$$\mathbf{L_1} = \frac{1}{\varepsilon_{33}\mu_{33} - \kappa^2}\begin{pmatrix} \mathbf{0_{2\times 2}} & \mathcal{P} \\ \mathcal{Q} & \mathbf{0_{2\times 2}} \end{pmatrix}, \tag{A2}$$

where

$$\mathcal{P} = \varepsilon_{33}\begin{pmatrix} -\mu_{23}\mu_{31} & -\mu_{23}\mu_{32} \\ \mu_{13}\mu_{31} & \mu_{13}\mu_{32} \end{pmatrix},$$

$$\mathcal{Q} = \mu_{33}\begin{pmatrix} \varepsilon_{23}\varepsilon_{31} & \varepsilon_{23}\varepsilon_{32} \\ -\varepsilon_{13}\varepsilon_{31} & -\varepsilon_{13}\varepsilon_{32} \end{pmatrix},$$

and

$$\mathbf{L_2} = \frac{\kappa}{\varepsilon_{33}\mu_{33} - \kappa^2}\begin{pmatrix} \mathcal{V} & \mathbf{0_{2\times 2}} \\ \mathbf{0_{2\times 2}} & \mathcal{W} \end{pmatrix}, \tag{A3}$$

where

$$\mathcal{V} = \begin{pmatrix} -\varepsilon_{31}\mu_{23} & -\varepsilon_{32}\mu_{23} \\ \varepsilon_{31}\mu_{13} & \varepsilon_{32}\mu_{13} \end{pmatrix},$$

$$\mathcal{W} = \begin{pmatrix} \varepsilon_{23}\mu_{31} & \varepsilon_{23}\mu_{32} \\ -\varepsilon_{13}\mu_{31} & -\varepsilon_{13}\mu_{32} \end{pmatrix}.$$

$\mathbf{L}'$, the corresponding matrix in the virtual space, can be easily found by substituting $\kappa = 0$. It is clear that $\mathbf{L}'$ is an antiblock diagonal matrix.

APPENDIX B: TRANSFORMATION FROM ISOTROPIC CHIRAL MEDIUM TO SIMPLE MEDIUM

Transformation between isotropic chiral medium and simple medium is expected; the relation of wave solutions between the virtual and physical spaces should be $\mathbf{F}' = \mathbf{R}\,\mathbf{F} + \mathbf{G}\,(E_z,\ E_z,\ Z_0H_z,\ Z_0H_z)^T$ in general, where the transformation matrices $\mathbf{R}(\omega, z)$ and $\mathbf{G}(\omega, z)$ are related to transverse and longitudinal components respectively. In a specific expression, $\mathbf{R}(\omega, z) = \mathbf{I}_{2\times 2} \otimes [[(\mathbf{A}^T)^{-1}]_{ab}]$, where $a, b = 1, 2$ and $\mathbf{A}$ is the transformation matrix in three-dimensional space. Since the propagation direction of EM waves is parallel to the z axis and the medium is homogeneous in x and y directions, it is not necessary to take a different transformation direction from the propagation direction. As a result, we can suppose $A_{13} = A_{23} = A_{31} = A_{32} = 0$, which induces $\mathbf{G} = \mathbf{0}$. By substituting the relation of solutions into Eq. (1), we get

$$\frac{d}{dz}\mathbf{F}' = \left[\frac{i\omega}{c}\mathbf{R}(\mathbf{M} + \mathbf{L_1})\mathbf{R}^{-1} - \left(\frac{\omega}{c}\mathbf{R}(\mathbf{K} + \mathbf{L_2})\mathbf{R}^{-1} + \mathbf{R}\frac{d}{dz}\mathbf{R}^{-1}\right)\right]\mathbf{F}'. \tag{B1}$$

If $\mathbf{L}$ is included, the transformation will become extremely complicated. For the sake of simplicity, we assume the permittivity and permeability in the virtual space are diagonal, homogeneous, and nondispersive so that $\mathbf{L} = \mathbf{0}$ and the wave solution in the virtual space is simply a plane wave. The operator in Eq. (4) is an antiblock diagonal matrix. Therefore, it is reasonable to say the block diagonal matrices in Eq. (B1) are contributed by the chirality, and it should be eliminated during the transformation, i.e.,

$$\frac{\omega}{c}\mathbf{K}\mathbf{R}^{-1} + \frac{d}{dz}\mathbf{R}^{-1} = \mathbf{0}. \tag{B2}$$

After solving the above differential matrix equation, we can get Eq. (5). By applying $d/dz = A_{33}d/dz'$, the differential matrix becomes

$$\frac{d}{dz'}\mathbf{F}' = \frac{1}{A_{33}}\left[\frac{i\omega}{c}\mathbf{R}\mathbf{M}\mathbf{R}^{-1}\right]\mathbf{F}'. \tag{B3}$$

By comparing the elements of

$$\boldsymbol{\varepsilon}'(z) = \frac{1}{\det\mathbf{A}}\mathbf{A}\boldsymbol{\varepsilon}(z)\mathbf{A}^T,$$

$$\boldsymbol{\mu}'(z) = \frac{1}{\det\mathbf{A}}\mathbf{A}\boldsymbol{\mu}(z)\mathbf{A}^T, \tag{B4}$$

and the elements of the operator in Eq. (B3) one by one, it is not difficult to notice that they match and A_{33} can be arbitrary.

APPENDIX C: PROPERTIES OF THE DISPERSION RELATIONS OF THE DESIGNED CHIRAL PHOTONIC CRYSTALS

The dispersion relation of the original chiral photonic crystal can be found by Eq. (9). By supposing $\alpha(a) = \theta(a) - \pi$,

where $\theta(a) \in (\pi, 2\pi)$, the dispersion relation is

$$\begin{aligned} e^{iv\pi}\mathbf{F}(\omega,0) &= \mathbf{R}^{-1}(\theta(a))\exp\left(\frac{i\omega a}{c}\mathbf{M}'\right)\mathbf{F}(\omega,0) \\ &= -\mathbf{R}^{-1}(\alpha(a))\exp\left(\frac{i\omega a}{c}\mathbf{M}'\right)\mathbf{F}(\omega,0) \\ &= e^{i(u\pm1)\pi}\mathbf{F}(\omega,0), \end{aligned}$$

where v and u are the normalized Bloch's vectors of the structural "twisted" angles are $\theta(a)$ and $\alpha(a)$ respectively. It is clear that the band structure of $\theta(a)$ can overlap with the band structure of $\theta(a)+\pi$ by shifting either one to the left (or right) by 1; also the eigenvectors follow the shifting. Similar results can be found in the regions $[0, \pi/2)$ and $[\pi/2, \pi)$; nevertheless, the eigenvectors do not follow the shifting. Let $\alpha(a) = \pi - \theta(a)$, where $\theta(a) \in (\pi/2, \pi]$. The dispersion relation is

$$\begin{aligned} e^{iv\pi}\mathbf{F}(\omega,0) &= \mathbf{R}^{-1}(\theta(a))\exp\left(\frac{i\omega a}{c}\mathbf{M}'\right)\mathbf{F}(\omega,0) \\ &= -\mathbf{R}(\alpha(a))\exp\left(\frac{i\omega a}{c}\mathbf{M}'\right)\mathbf{F}(\omega,0) \\ &\neq -\mathbf{R}^{-1}(\alpha(a))\exp\left(\frac{i\omega a}{c}\mathbf{M}'\right)\mathbf{F}(\omega,0) \\ &= e^{i(u\pm1)\pi}\mathbf{F}(\omega,0). \end{aligned}$$

Although the results do show the normalized Bloch vectors $u \pm 1$ equals v, this cannot ensure the eigenvectors are the same. Therefore, the region $\theta(a) \in [0, \pi]$ is mainly focused in this study.

APPENDIX D: PROPERTIES OF THE TRANSFORMED STRUCTURE

1. Chirality parameter in the transformed structure

Maxwell's equations in the transformed structure can be expressed as

$$\frac{d}{dz}\mathbf{F}'' = \left[\frac{i\omega}{c}\mathbf{R}\mathbf{M}\mathbf{R}^{-1} - \left(\frac{\omega}{c}\mathbf{R}\mathbf{K}\mathbf{R}^{-1} + \mathbf{R}\frac{d}{dz}\mathbf{R}^{-1}\right)\right]\mathbf{F}'. \tag{D1}$$

$\mathbf{R}(z)$ is continuous through whole space because $\theta(z)$ is replaced by $\phi(z)$. Again, the second term in the square brackets should be contributed by chirality; the chirality parameter in the transformed structure is

$$\kappa'' = \frac{d\phi}{dz} - \frac{\omega}{c}\kappa(\omega, z) = \frac{d\phi}{dz} - \frac{\theta_{\max}}{a},$$

where $\theta_{\max} = \lim_{z\to a^+}\theta(z) \doteq \theta(a)$. Because of $\phi(z) = \theta_{\max} z/a$ according to the Eq. (10), the above equation becomes

$$\kappa'' = \frac{d\phi}{dz} - \frac{\theta_{\max}}{a} = 0. \tag{D2}$$

Therefore, the chirality parameter becomes zero in the transformed structure. The remaining parts in Eq. (D1) stand for the permittivity and permeability parameters in the transformed structure, which are expressed in Eq. (14) when $\theta(a) = \pi/2$ is chosen. The proof is trivial and omitted.

2. Separating two independent modes

When the structural "twisted" angle $\theta(a)$ is chosen to be $\pi/2$, the transformed structure is a simple anisotropic binary photonic crystal, which is shown in Fig. 2. If $\mathbf{F}''$ is rearranged in the form $(E''_{x''},\ Z_0 H''_{y''},\ E''_{y''},\ -Z_0 H''_{x''})^T = (|\psi_{x''}\rangle,\ |\psi_{y''}\rangle)^T$ and the white and black slabs are named as A and B slabs respectively, the matrices $\mathbf{M}''$ of white and black slabs are

$$\mathbf{M}''_w = \begin{pmatrix} 0 & \mu'_{22} & 0 & 0 \\ \varepsilon'_{11} & 0 & 0 & 0 \\ 0 & 0 & 0 & \mu'_{11} \\ 0 & 0 & \varepsilon'_{22} & 0 \end{pmatrix} \equiv \mathbf{X} \oplus \mathbf{Y} \tag{D3}$$

and

$$\mathbf{M}''_b = \begin{pmatrix} 0 & \mu'_{11} & 0 & 0 \\ \varepsilon'_{22} & 0 & 0 & 0 \\ 0 & 0 & 0 & \mu'_{22} \\ 0 & 0 & \varepsilon'_{11} & 0 \end{pmatrix} \equiv \mathbf{Y} \oplus \mathbf{X}, \tag{D4}$$

where the subscripts w and b represent white and black slabs respectively. The symbol $\oplus$ is the direction sum, for example, $\mathbf{X} \oplus \mathbf{Y} = \mathrm{diag}(\mathbf{X}, \mathbf{Y})$. $|\psi_{x''}\rangle$ and $|\psi_{y''}\rangle$ modes can be calculated individually since the operator is block diagonal now. The dispersion relations of $|\psi_{x''}\rangle$ and $|\psi_{y''}\rangle$ modes are

$$e^{ik''_z\Lambda}|\psi_{x''}\rangle = \exp\left(\frac{i\omega a}{c}\mathbf{Y}\right)\exp\left(\frac{i\omega a}{c}\mathbf{X}\right)|\psi_{x''}\rangle, \tag{D5a}$$

$$e^{ik''_z\Lambda}|\psi_{y''}\rangle = \exp\left(\frac{i\omega a}{c}\mathbf{X}\right)\exp\left(\frac{i\omega a}{c}\mathbf{Y}\right)|\psi_{y''}\rangle, \tag{D5b}$$

where $\Lambda = 2a$. There is a remark that the matrices $\mathbf{M}$ in isotropic binary photonic crystals are $\mathbf{M}_w = \mathbf{X} \oplus \mathbf{X}$ and $\mathbf{M}_b = \mathbf{Y} \oplus \mathbf{Y}$; thus, the eigenvectors of $|\psi_x\rangle$ and $|\psi_y\rangle$ are the same and only either one of the modes needs considering. Furthermore, the transformed anisotropic binary photonic crystal can be regarded as XY and YX isotropic layered photonic crystals if $|\psi_{x''}\rangle$ and $|\psi_{y''}\rangle$ are individually considered.

3. Relation of the Bloch vectors in original and transformed structures

If $\mathbf{F}$ is also rearranged in the form $(E_x,\ Z_0 H_y,\ E_y,\ -Z_0 H_x)^T \doteq (|\psi_x\rangle,\ |\psi_y\rangle)^T$, the operator in Eq. (9) can be written as

$$\begin{aligned} &\mathbf{R}^{-1}(a)\exp\left(\frac{i\omega a}{c}\mathbf{M}'\right) \\ &= \left[\mathbf{I}_{2\times2} \otimes \begin{pmatrix} 0 & -1 \\ 1 & 0 \end{pmatrix}\right]\exp\left(\frac{i\omega a}{c}(\mathbf{X} \oplus \mathbf{Y})\right). \end{aligned} \tag{D6}$$

The dispersion relations of $|\psi_x\rangle$ and $|\psi_y\rangle$ modes are

$$e^{ik_z a}|\psi_x\rangle = -\exp\left(\frac{i\omega a}{c}\mathbf{Y}\right)|\psi_y\rangle$$

$$e^{ik_z a}|\psi_y\rangle = \exp\left(\frac{i\omega a}{c}\mathbf{X}\right)|\psi_x\rangle,$$

which implies

$$e^{2ik_z a\pm\pi}|\psi_x\rangle = \exp\left(\frac{i\omega a}{c}\mathbf{Y}\right)\exp\left(\frac{i\omega a}{c}\mathbf{X}\right)|\psi_x\rangle, \quad \text{(D7a)}$$

$$e^{2ik_z a\pm\pi}|\psi_y\rangle = \exp\left(\frac{i\omega a}{c}\mathbf{X}\right)\exp\left(\frac{i\omega a}{c}\mathbf{Y}\right)|\psi_y\rangle. \quad \text{(D7b)}$$

By comparing Eqs. (D5) and (D7), the eigenvectors $|\psi_x(k_z\Lambda/\pi \pm 1)\rangle$ and $|\psi_y(k_z\Lambda/\pi \pm 1)\rangle$ equal $|\psi_{x''}(k_z'')\rangle$ and $|\psi_{y''}(k_z'')\rangle$ respectively, and the relation of the eigenvalue is

$$\frac{k_z\Lambda}{\pi} = \frac{k_z''\Lambda}{\pi} + (2s-1), \quad \text{(D8)}$$

where s is an integer for controlling the wave vector within the range of $[-1,1]$.

[1] J. B. Pendry, D. Schurig, and D. R. Smith, Controlling electromagnetic fields, Science **312**, 1780 (2006).

[2] U. Leonhardt, Optical conformal mapping, Science **312**, 1777 (2006).

[3] Y. Lai, J. Ng, and C. T. Chan, Creating illusion effects using transformation optics, in *Transformation Electromagnetics and Metamaterials*, edited by D. H. Werner and D.-H. Kwon (Springer, 2014), pp. 139–165.

[4] H. Chen, C. T. Chan, and P. Sheng, Transformation optics and metamaterials, Nat. Mater. **9**, 387 (2010).

[5] D.-H. Kwon and D. H. Werner, Polarization splitter and polarization rotator designs based on transformation optics, Opt. Express **16**, 18731 (2008).

[6] P. A. Huidobro, M. L. Nesterov, L. Martín-Moreno, and F. J. García-Vidal, Transformation optics for plasmonics, Nano Lett. **10**, 1985 (2010).

[7] Y. Zhang, L. Shi, R. Y. Zhang, J. Duan, J. Ng, C. T. Chan, and K. H. Fung, Metric-Torsion Duality of Optically Chiral Structures, Phys. Rev. Lett. **122**, 200201 (2019).

[8] L. Lu, J. D. Joannopoulos, and M. Soljačić, Topological photonics, Nat. Photon. **8**, 821 (2014).

[9] A. B. Khanikaev, S. H. Mousavi, W.-K. Tse, M. Kargarian, A. H. MacDonald, and G. Shvets, Photonic topological insulators, Nat. Mater. **12**, 233 (2013).

[10] Y. Z. Yu, C. Y. Kuo, R. L. Chern, and C. T. Chan, Photonic topological semimetals in bianisotropic metamaterials, Sci. Rep. **9**, 1 (2019).

[11] M. Xiao, Z. Q. Zhang, and C. T. Chan, Surface impedance and bulk band geometric phases in one-dimensional systems, Phys. Rev. X **4**, 021017 (2014).

[12] K. H. Choi, C. W. Ling, K. F. Lee, Y. H. Tsang, and K. H. Fung, Simultaneous multi-frequency topological edge modes between one-dimensional photonic crystals, Opt. Lett. **41**, 1644 (2016).

[13] K. H. Fung, J. C. W. Lee, and C. T. Chan, Chiral photonic and plasmonic structures, in *Plasmonics and Plasmonic Metamaterials: Analysis and Applications* (World Scientific, Singapore, 2011), Chap. 2.

[14] C. W. Oseen, The theory of liquid crystals, Trans. Faraday Soc. **29**, 883 (1933).

[15] H. Rhee, Y.-G. June, J.-S. Lee, K.-K. Lee, J.-H. Ha, Z. H. Kim, S.-J. Jeon, and M. Cho, Femtosecond characterization of vibrational optical activity of chiral molecules, Nature (London) **458**, 310 (2009).

[16] I. Bita and E. L. Thomas, Structurally chiral photonic crystals with magneto-optic activity: Indirect photonic bandgaps, negative refraction, and superprism effects, J. Opt. Soc. Am. B **22**, 1199 (2005).

[17] A. H. Sihvola, A. J. Viitanen, I. V. Lindell, and S. A. Tretyakov, *Electromagnetic Waves in Chiral and Bi-Isotropic Media* (Artech House Antenna Library, Norwood, MA, 1994).

[18] O. Ortiz, P. Priya, A. Rodriguez, A. Lemaitre, M. Esmann, and N. D. Lanzillotti-Kimura, Topological optical and phononic interface mode by simultaneous band inversion, Optica **8**, 598 (2021).

[19] L. Gilles and P. Tran, Optical switching in nonlinear chiral distributed Bragg reflectors with defect layers, J. Opt. Soc. Am. B **19**, 630 (2002).

[20] D. Smirnova, D. Leykam, Y. Chong, and Y. Kivshar, Nonlinear topological photonics, Appl. Phys. Rev. **7**, 021306 (2020).

[21] D. L. Mills and S. E. Trullinger, Gap solitons in nonlinear periodic structures, Phys. Rev. B **36**, 947 (1987).